Energy Proceedings
Vol 36, 2023
ISSN 2004-2965

Investigation of Methane Seepage and Geochemical Indicators in Porewater in "Haima" Cold Seep, South China Sea

Li Tang[1,2], Jing-Chun Feng[1,2*], Hui Zhang[1,2], Canrong Li[1,2], Si Zhang [1,2]

1 Institute of Environmental and Ecological Engineering, Guangdong University of Technology, Guangzhou 510006, China

2 Southern Marine Science and Engineering, Guangdong Laboratory (Guangzhou), Guangzhou 511458, China
(*Corresponding Author: fengjc18@163.com)

ABSTRACT

Geochemical characterization of seafloor sediment porewater as a rapid response to methane seepage and its biogeochemical processes to document methane seepage characteristics. In this study, methane seepage and geochemical indicators in porewater were investigated for five stations in "Haima" Cold Seep in the South China Sea. The results showed that the methane release in different stations was quite different, with the methane diffusion flux ranged from 0.3 to 168.3 μmol/(m²·a). However, there were some similarities in the geochemical indicators for every station. Correlation analysis indicated that methane seepage was positively correlated with depth and PO_4^{3-}, and negatively correlated with TS, K^+, Na^+, Mg^{2+}, Mn^{2+}, Fe^{3+}, and NO_2^-. The PCA cluster analysis results were similar to the classification of habitat characteristics observed during sampling. Therefore, it may be possible to provide an indication of methane leakage through habitat characteristics in future studies.

Keywords: cold seep, methane seepage, sediment, geochemical characteristics

1. INTRODUCTION

Methane (CH_4) is one of the important greenhouse gases, its single -molecule absorbing infrared radiation is more than 20 times higher than carbon dioxide, which plays an important role in global warming and atmospheric chemistry. In addition, the contribution to the greenhouse effect by methane can reach 20% [1]. Methane production activities in seawater and methane emissions from marine sediments are important natural sources of methane emissions. In addition, oceans cover more than 70% of the Earth's surface, and marine sediments are the largest methane reservoirs [2]. Therefore, the oceans contribute significantly to the global methane budget for atmospheric methane concentrations in all natural sources of methane emissions [3]. Moreover, the release of methane from the oceans has been closely linked to sudden increases in temperature and five mass extinctions in Earth's history [4], which requires a deep understanding of the underlying and corresponding control factors for ocean methane emissions [5, 6].

Seafloor methane seepage refers to the process which fluids rich in hydrocarbons (mainly CH_4) are transported upwards from deep or shallow seafloor along high-permeability channels such as fractures and faults and porous media in the form of seepage or outflow. The released methane mainly comes from in-situ conversion of organic carbon, decomposition of deeply buried natural gas hydrates or oil and gas leaks [2, 7]. As a marker of natural gas hydrate and an important way for its decomposition to release methane, cold seep activity has triggered extremely complex biogeochemical processes at the seawater sediment interface, for example, sulfate-driven methane anaerobic oxidation reaction (SD-AOM, equation (1)), and Sulfate reduction reaction (OSR, equation (2)). Among them, studies have shown that nearly 90% of seafloor seepage methane is consumed by anaerobic oxidation (AOM) and fails to be released into the atmosphere [3]. Therefore, cold seep activities thus have a significant impact on the global methane carbon cycle and climate change. In recent years, scientists have carried out a great deal of work on seafloor cold seep activities. However, there are still some uncertainties in the estimation of methane fluxes from seafloor cold seeps and in the geochemical signatures of the transport processes due to differences in the estimation of the study samples and the limitations of the technical means of observation.

$$\mathrm{CH_4} + SO_4^{2-} \rightarrow HS^- + HCO_3^- + H_2O \quad (1)$$

$$2\mathrm{CH_2}O + SO_4^{2-} \rightarrow 2HCO_3^- + H_2S \quad (2)$$

This is a paper for the 9th Applied Energy Symposium: Low Carbon Cities and Urban Energy Systems (CUE2023), Sep. 2-7, 2023, Matsue & Tokyo, Japan.

Porewater is a liquid-phase fluid that exists in the pores of solid-phase sediments. The study of the geochemistry of sediment porewater is an important indicator of early diagenesis, redox environmental changes, fluid sources and transport processes, and microbial geochemistry of the surface layer [8-10]. The "Haima" cold seep in the northern part of the South China Sea is the second active methane cold seep discovered in China, with high resource reserves. Based on this, this study investigated the vertical transport and transformation patterns of methane and sulphate in porewater and calculated their diffusive fluxes in “Haima” cold seep. Meanwhile, we also studied the relationship between methane seepage and geochemical indicators by correlation analysis and PCA analysis. It is hoped that the results of this study can provide scientific references for tracking methane seepage in sediments around the world.

2. MATERIALS AND METHODS

2.1 Background of the study area

“Haima” cold seep is located in the southwestern part of Qiongdongnan Basin (16°43’N, 110°28’E), and the cold seep area is generally spreading in the shape of EW strip, with an area of about 618 km^2, among which the area with cold seeo activity has been found to be about 350 km^2. The water depth of the investigated area is from 1,350 to 1,430 m, and the terrain is relatively gentle, with a gentle slope that gradually becomes deeper and deeper from southwestern to northeastern, and the slope degree is about 0.2°. “Haima” cold seep is the first active cold seep of unprecedented scale discovered by China in the western part of the northern land slope of the South China Sea, and its discovery is a major breakthrough in the exploration of natural gas hydrate.

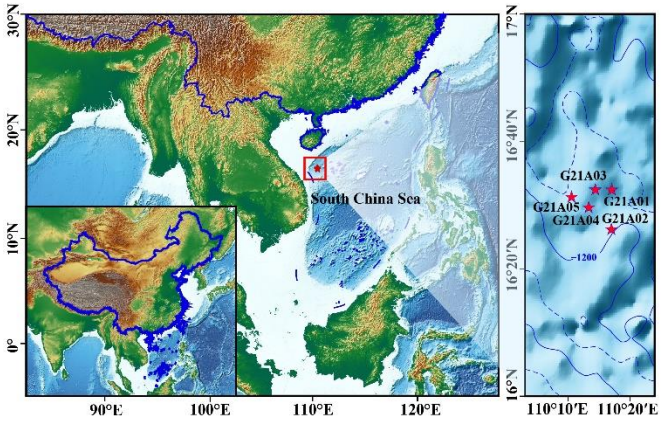

Fig.1 Distribution of the study are*a*

2.2 Sample collection and preparation

The scientific expedition will take place in May 2021 aboard the "Haiyangdizhi VI". The studied sediment column samples were obtained using large gravity piston samplers, and the sample information is shown in Fig. 1, with the water depths of 1441, 1483, 1366, 1394, and 1372 m and gravity column lengths of 725, 675, 775, 825, and 675 cm for G21A01-G21A05, respectively. During sampling, a large number of methane bubbles were observed seeping from the station of G21A01, and there were several mussel colonies, white clams, anemones, Ophiuroidea and other organisms, as well as small pieces of carbonate rocks on the sediments. The station of G21A02 did not find the methane bubble leakage, but there were tubeworms, mussels, anemones and other organisms, and with a large carbonate rock, which is richer than that of G21A01. At G21A03, trace methane bubble seepage can be observed, with white clams, anemones, and white attachments suspected to be fungal mats on the sediment surface. However, there were no obvious habitat features had found in the station of G21A04 and G21A05.

After sampling, sediment columns were cut into 1 m, the top and bottom of the columns were closed using plastic caps with tape and placed horizontally. Holes were drilled at 10-20 cm intervals using an electric drill rig, followed by porewater collection using Rhizon with a 0.2 μm filter membrane. All porewater samples collected were divided into two parallel samples, one for methane testing and the other for geochemical indicator testing. All porewater samples were stored in a refrigerator at 4°C for further analysis.

2.3 Geochemical indicators testing and diffusive flux calculations

The major elements (Na^+, K^+, Ca^{2+}, Mg^{2+}) in porewater were measured using inductively coupled plasma spectrometry (ICAP-7200, Thermo Fisher Scientific). Trace elements (Mn^{2+}, Ba^{2+}, Sr^{2+}) were tested by inductively coupled plasma mass spectrometer (iCAP Q, Thermo Fisher Scientific). Cl^- and SO_4^{2-} were tested using an ion chromatograph (AQ-1200, Thermo Fisher Scientific). Total Organic Carbon (TOC) and inorganic carbon (IC) were analyzed by total organic carbon analyzer (TOC-L). Nutrient salts (SiO_3^{2-}, PO_4^{3-}, NO_2^-, NO_3^-, NH_4^+) were measured by GB/T12763.4-2007. Methane concentration was tested using gas chromatograph (Thermo Fisher Scientific).

The molecular diffusion fluxes of methane and sulfate in porewater are calculated using Fick's first law [2, 8], as shown in equations (3) and (4).

$$J = -\varphi D_s \frac{\partial C}{\partial x} \quad (3)$$

$$D_s = \frac{D_0}{1-\ln \varphi^2} \quad (4)$$

J is methane or sulfate diffusion flux (mmol/(m^2·a)). ψ is the porosity, which estimated to be 65%. Ds is the sediment diffusion coefficient (m^2/s). *C* is the concentration of methane or sulfate (mmol/L). *x* is the depth of the sediment (m). *Do* is the diffusion coefficient of methane or sulfate at a seawater temperature of 4°C, in this study, the diffusive flux was taken as 0.87×10^{-5} cm^2/s for methane, and 0.56×10^{-5} cm^2/s for sulfate [11].

2.4 Statistical analysis

Principal component analysis (PCA) is a multivariate statistical analysis technique in which a set of correlated variables is transformed into a new set of mutually uncorrelated or orthogonal variables [12]. In this study, PCA was used to estimated the relationship of CH_4 concentration and geochemical indicators. Pearson Correlation is a measure of vector similarity, and in this study, Pearson correlation analysis also be used to measure the correlation between methane and geochemical indicators.

3. RESULTS AND DISCUSSION

3.1 *The vertical distribution of geochemical indicators*

As shown in Fig.2a, the IC concentration is higher than the TOC concentration in five stations. In the depth of 0-200 cm, the stations of G21A01-G21A03 showed a slight decreasing trend in TOC concentration and then showed a significant increase deeper than 200 cm. While an opposite trend was showed in stations of G21A04 and G21A05, in the depth of 0-100 cm, there showed a slight increase in TOC concentration and then slightly decreased in the depth of 100-200 cm, followed by a rapid increasing trend after 400 cm. For IC, it can be found that stations of G21A01-G21A04 tend to stabilize in the range of 0-400 cm and rapidly increase in depth below 400 cm. While station G21A05 was stabilized in the range of 0-100 cm and showed a clear increasing trend below 100 cm depth.

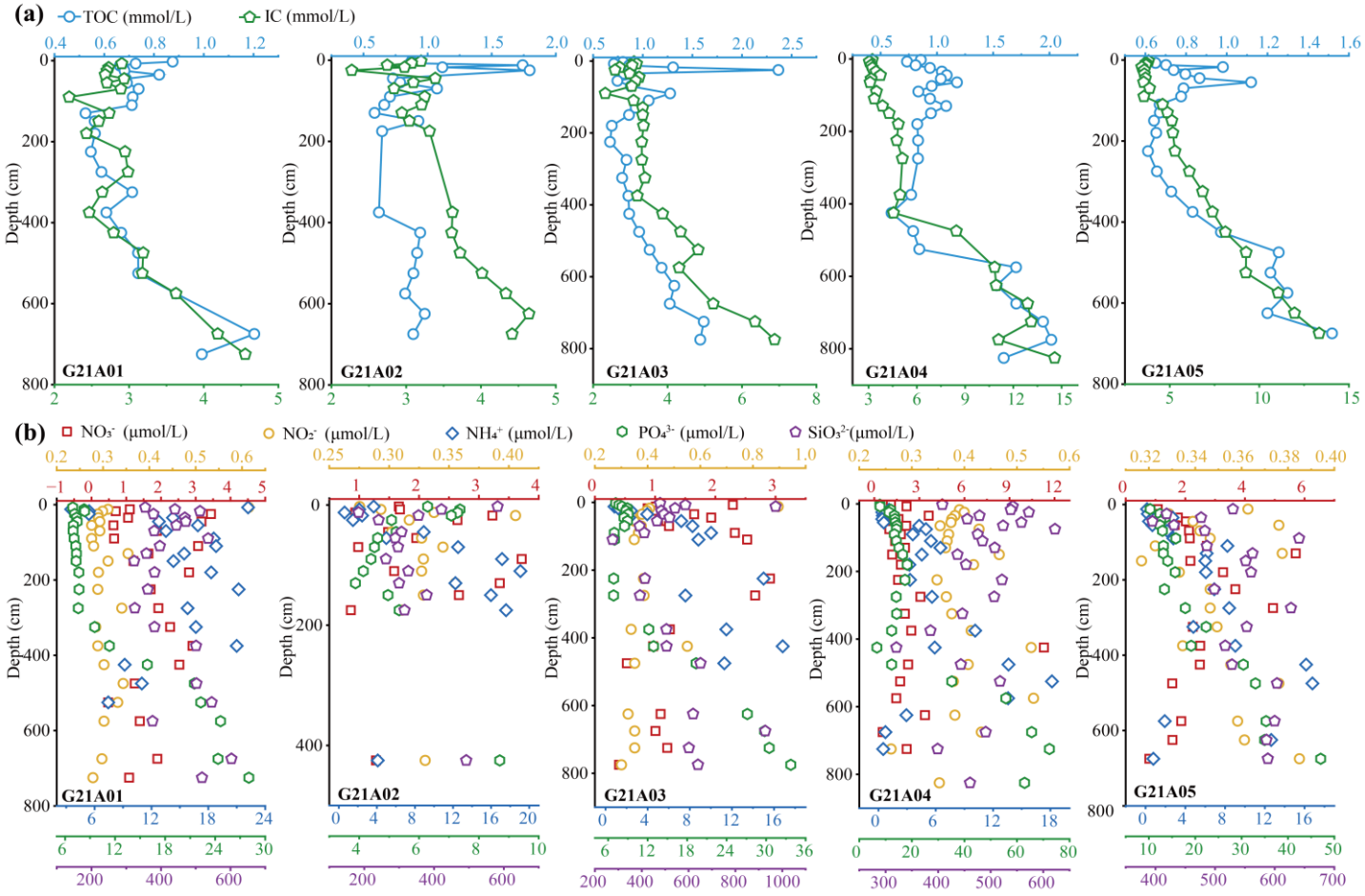

Fig.2 Vertical distribution of geochemical indicators. (a) TOC and IC. (b) Nutrient salt (NO_3^-、NO_2^-、NH_4^+、PO_4^{3-}、SiO_3^{2-})

The distribution of nutrient salts (NO_2^-, NO_3^-, NH_4^+, PO_4^{3-}, SiO_3^{2-}) was shown in Fig.2b. It can be found that there is no significant difference in the distribution of nutrient salts among five stations. Among them, the concentration of NO_2^- was all ranged from 0.2 to 0.6 mmol/L, with no significant trend; NO_3^- concentrations at

stations G21A03 and G21A05 showed a slight trend of increasing and then decreasing, while the other of the stations showed no obvious trend. Except for G21A02 which lacked nutrient salts concentration due to the lack of samples, NH_4^+ and PO_4^{3-} concentrations at the remaining four stations showed an overall trend of increasing with depth trend, while the SiO_3^{2-} showed an overall trend of decreasing and then increasing.

3.2 CH_4 and sulfate in different stations in the "Haima" cold seep

The distribution of methane and sulfate concentrations in porewater were shown in the Fig.3. It can be found that, for station G21A01, the methane concentration showed no obvious change in the depth of 0-400 cm, while the sulfate concentration decreased from 19.07 mmol/L to 15.04 mmol/L. It is presumed that sulfate reduction reaction took place in this depth range. In the depth of 400-500 cm, the methane concentration showed an obvious increasing trend, and the sulfate concentration continued to show a slight decrease. Therefore, it is presumed that SD-AOM occurred in this depth range. As the depth continued to increase, the methane concentration continued to increase, and the increase in methane concentration is generally generated by the decomposition of hydrates or biological methanogenesis. During the sampling, the station of G21A01 was observed to have obvious methane bubbles leakage, therefore, it is assumed that methane is produced by hydrate decomposition. At the same time, the disturbance of a large number of methane bubbles seepage led to fluctuation of sulfate after 400 cm. For the station of G21A02, the methane concentration increased slightly in the range of 0.4-0.8 μmol/L, and the sulfate concentration fluctuated slightly only in the concentration of 14-18 mmol/L. Due to the lack of corresponding geochemical indicators data for G21A02, it is hypothesized based on the habitat information that this may be a late stage in the development of the cold seep. Therefore, the AOM activity was weak, and the OSR was dominated. For stations of G21A03 and G21A04, methane concentration did not change significantly in the depth of 0-500 cm, while sulfate showed a slow decreasing trend at this range. It was hypothesized that OSR was occurring in this stage, whereas in the depth of 500-800 cm, the trend of methane elevation gradually increased, while the trend of decreasing sulfate concentration tended to be obvious, and thus a SD-AOM might have occurred at this stage. For the station of G21A05, the methane concentration showed a little change, while the sulfate concentration showed a trend of decrease. Therefore, it is presumed that the station is mainly dominated by the OSR, while the AOM plays only a weak role.

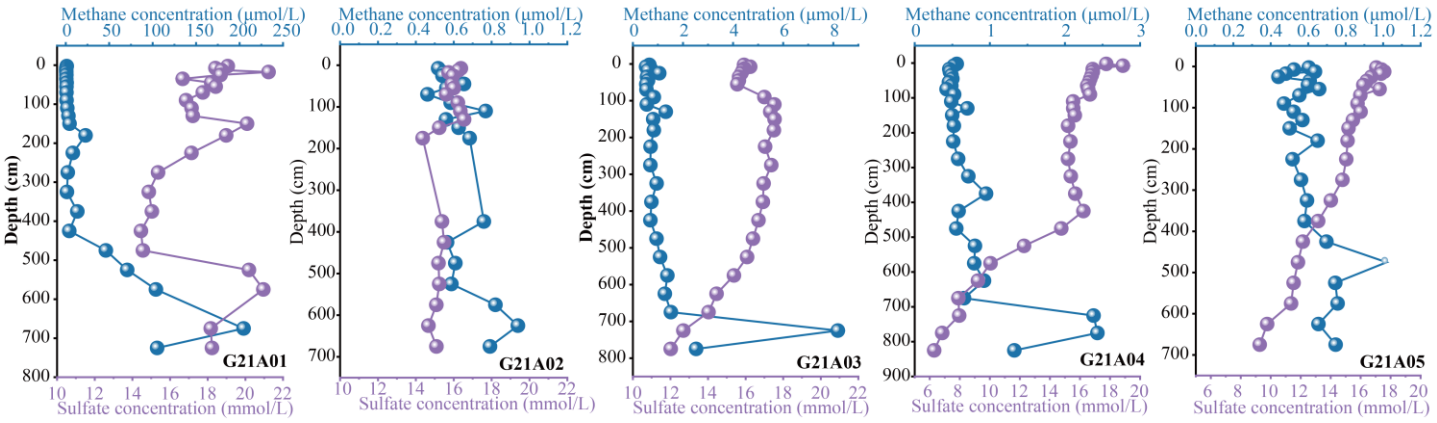

Fig. 3 Vertical distribution of methane/sulfate concentrations

Table. 1 Calculation of methane and sulfate diffusive fluxes in porewater

J (μmol/(m²·a))	G21A01	G21A02	G21A03	G21A04	G21A05
CH_4	168.3	0.3	3.1	3.1	4.0
SO_4^{2-}	785.6	1087.8	2831.6	7736.3	6904.5

In addition, as shown in Table.1, we also calculated the diffusive fluxes of methane and sulfate in the porewater. It can be found that the minimum methane diffusive flux was 0.3 μmol/(m²·a) at the station of G21A02, while the maximum methane diffusive flux was 168.3 μmol/(m²·a) at station of G21A01, where a large amount of methane leakage was observed. The opposite result was showed for sulfate diffusion fluxes, with the smallest sulfate diffusion flux of 785.6 μmol/(m²·a) at station G21A01. It is interesting to note that, there is no special habitats were

detected at stations G21A04 and G21A05 during sampling, while their sulfate diffusion fluxes were the largest, with 7736.3 μmol/(m²·a) and 6904.5 μmol/(m²·a), the reasons for this need in-depth analysis.

It can be seen that though the five stations are in the same cold seep area, there are large differences in their methane concentrations and vertical migration characteristics. Therefore, we need to cover as many sampling stations as possible when conducting the global assessment of methane concentrations in sediments, so that the assessment results can be more accurate.

3.3 Correlation analysis between geochemical indicators and methane seepage

As shown in Fig. 4, it can be found that methane concentration in the porewater showed significant positive correlation with depth and PO_4^{3-}, and showed significant negative correlation with TS, K^+, Na^+, Mg^{2+}, Mn^{2+}, Fe^{3+}, and NO_2^-. The negative correlation between methane concentration and Mn^{2+}, Fe^{3+}, and NO_2^- once again verified that anaerobic oxidation of methane can use it as an electron acceptor.

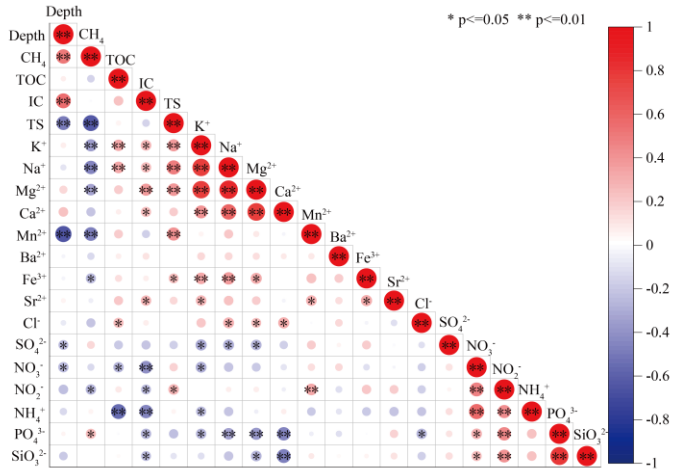

Fig. 4 Correlation analysis between environmental factors and methane seepage

The PCA analysis in Fig. 5 shows that station G21A01 is little similar to the other stations, G21A02 has a strong similarity to G21A03, and station G21A04 has a strong similarity to G21A05 with the exception of some points. This performance is similar to the classification of the phenomena observed in habitats characteristics, which suggests that the geochemical indicators have a strong indication of habitat characteristics. Meanwhile, it can be found that the geochemical indicators of the five stations are mainly divided into 3 categories (PC1: 25.1%, PC2: 18.6%, PC3: 10.3%), of which the first principal component is mainly composed of depth, IC, TS, SO_4^{2-} and PO_4^{3-}, the load coefficients are 0.34, 0.42, -0.38, -0.36 and 0.41. The second principal component is mainly composed of K^+, Na^+, Mg^{2+}, and Mn^{2+}, the load coefficient is 0.42, 0.38, 0.43 and 0.39, respectively. The third principal component is mainly composed of Mg^{2+}, Ca^{2+}, Cl^-, and NH_4^+, and the load coefficients are 0.30, 0.31, -0.34 and 0.43, respectively.

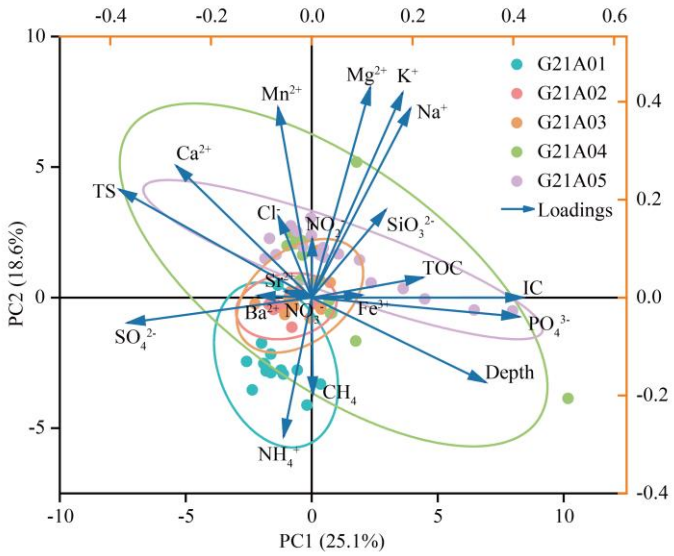

Fig. 5 Principal component analysis of environmental factors and methane seepage

In addition, combined with the distribution characteristics of TOC, IC and nutrient salts in Fig. 2, it can be found that there exists a certain relationship between TOC, IC and the change of methane concentration, but the change of TOC and IC not only involves AOM and OSR, but also microbial chemoenergetic synthesis and mineralization, so the relationship between TOC, IC and methane leakage is worthy of in-depth analysis. Meanwhile, the changes of each ion in the nutrient salts also have a great relationship with the changes of methane, therefore, the indicative role of environmental factors on methane seepage deserves in-depth study by scholars in the subsequent research.

Table. 2 Loading of different geochemical indicators

Component	Component matrix		
Loadings	PC1	PC2	PC3
Depth	**0.34**	-0.17	0.18
CH_4	0.00	-0.20	-0.11
TOC	0.22	0.04	**-0.36**
IC	**0.42**	0.00	0.09
TS	**-0.38**	0.22	0.07
K^+	0.18	**0.42**	0.07
Na^+	0.19	**0.38**	0.19
Mg^{2+}	0.12	**0.43**	**0.30**
Ca^{2+}	-0.27	0.27	**0.31**
Mn^{2+}	-0.07	**0.39**	-0.26
Ba^{2+}	-0.11	0.00	-0.21
Fe^{3+}	0.10	0.01	0.06

Sr^{2+}	-0.05	0.01	-0.19
Cl^-	-0.07	0.16	**-0.34**
SO_4^{2-}	**-0.36**	-0.05	-0.09
NO_3^-	-0.05	0.01	0.29
NO_2^-	0.00	0.12	-0.06
NH_4^+	-0.06	-0.28	**0.43**
PO_4^{3-}	**0.41**	-0.04	-0.10
SiO_3^{2-}	0.15	0.18	-0.16

4. CONCLUSIONS

Cold seeps are environments where methane-rich fluids seep rapidly to the seafloor and produce a range of biogeochemical reactions. In this study, the vertical transport and transformation patterns of methane and sulphate in porewater were investigated in “Haima” cold seep. Meanwhile, we calculated their diffusive fluxes. Moreover, the relationship between methane seepage and geochemical indicators were analyzed by correlation analysis and PCA analysis. The results showed that there was no significant difference in TOC and IC among the five stations, and the concentrations of TOC and IC increased slowly at the beginning, and then rapidly with the increase of depth. Among the nutrient salt concentrations, there was no significant change in the concentration of NO_2^-, the concentration of NO_3^- showed a slight increase and then a decrease, and the concentrations of NH_4^+, PO_4^{3-}, and SiO_3^{2-} increased with the increase of depth. However, even in the same cold seep environment, methane and sulfate variations varied considerably from station to station, with the maximum of methane diffusive flux was 168.3 μmol/(m²·a) at station G21A01, and the minimum of methane diffusive flux was 0.3 μmol/(m²·a) at station G21A02. In addition, the correlation analysis could find that methane leakage showed a significant positive correlation with depth and PO_4^{3-}, and a significant negative correlation with TS, K^+, Na^+, Mg^{2+}, Mn^{2+}, Fe^{3+}, and NO_2^-. Meanwhile, the PCA analysis showed that the classification was similar to the classification of habitat characteristics observed during sampling. Therefore, in future studies, it may be possible to provide an indication of methane seepage through habitat information.

ACKNOWLEDGEMENT

The authors would like to acknowledge the financial support from the National Key Research and Development Program (2021YFF0502300), the National Natural Science Foundation of China (42022046, 42227803, 52122602, 41890850), the Guangdong Natural Resources Foundation, (GDNRC[2022]45, GDNRC[2023]30), and the PI project of Southern Marine Science and Engineering Guangdong Laboratory (Guangzhou) (GML20190609 and GML2022009).

DECLARATION OF INTEREST STATEMENT

The authors declare that they have no known competing financial interests or personal relationships that could have appeared to influence the work reported in this paper. All authors read and approved the final manuscript.

REFERENCE

[1] Stocker TF, D. Qin, G.-K. Plattner, M. Tignor, S.K. Allen, J. Boschung, A. Nauels, Y. Xia, V. Bex and P.M. Midgley. Climate Change 2013: The Physical Science Basis. ICPP. 2013.

[2] Egger M, Riedinger N, Mogollón JM, Jørgensen BB. Global diffusive fluxes of methane in marine sediments. Nature Geoscience. 2018;11:421-5.

[3] Reeburgh WS. Oceanic Methane Biogeochemistry. Chemical Reviews. 2007;107:486-513.

[4] Weldeab S, Schneider RR, Yu J, Kylander-Clark A. Evidence for massive methane hydrate destabilization during the penultimate interglacial warming. Proceedings of the National Academy of Sciences. 2022;119:e2201871119.

[5] Wang F, Harindintwali JD, Wei K, Shan Y, Mi Z, Costello MJ, et al. Climate change: Strategies for mitigation and adaptation. The Innovation Geoscience. 2023;1:100015.

[6] Feng J-C, Yan J, Wang Y, Yang Z, Zhang S, Liang S, et al. Methane mitigation: Learning from the natural marine environment. The Innovation. 2022;3:100297.

[7] Joye SB, Boetius A, Orcutt BN, Montoya JP, Schulz HN, Erickson MJ, et al. The anaerobic oxidation of methane and sulfate reduction in sediments from Gulf of Mexico cold seeps. Chemical Geology. 2004;205:219-38.

[8] Hu Y, Feng D, Peckmann J, Gong S, Liang Q, Wang H, et al. The impact of diffusive transport of methane on pore-water and sediment geochemistry constrained by authigenic enrichments of carbon, sulfur, and trace elements: A case study from the Shenhu area of the South China Sea. Chemical Geology. 2020;553:119805.

[9] Zindorf M, März C, Wagner T, Gulick SPS, Strauss H, Benowitz J, et al. Deep Sulfate-Methane-Transition and sediment diagenesis in the Gulf of Alaska (IODP Site U1417). Marine Geology. 2019;417:105986.

[10] Hong WL, Pape T, Schmidt C, Yao H, Wallmann K, Plaza-Faverola A, et al. Interactions between deep formation fluid and gas hydrate dynamics inferred from pore fluid geochemistry at active pockmarks of the Vestnesa Ridge, west Svalbard margin. Marine and Petroleum Geology. 2021;127:104957.

[11] Iversen N, Jørgensen BB. Diffusion coefficients of sulfate and methane in marine sediments: Influence of porosity. Geochimica et Cosmochimica Acta. 1993;57:571-8.

[12] Lever J, Krzywinski M, Altman N. Principal component analysis. Nature Methods. 2017;14:641-2.